Antarctic Science 7 (1): 63–72 (1995)

Geochemistry of a fossil hydrothermal system at Barton Peninsula, King George Island

CHIL-SUP SO[1], SEONG-TAEK YUN[2] and MAENG-EON PARK[3]

[1]Department of Earth and Environmental Science, Korea University, Seoul 136-701, Korea
[2]Department of Mineral and Energy Resources Engineering, Semyung University, Jecheon 390-230, Korea
[3]Department of Applied Geology, Pusan National Fisheries University, Pusan 608-737, Korea

Abstract: A fossil hydrothermal system on Barton Peninsula, King George Island, Antarctica, formed a series of lead-zinc- and pyrite + native sulphur-bearing epithermal quartz ± calcite veins, filling fault-related fractures in hydrothermally altered volcanic rocks of Eocene age. The lead-zinc veins occur within argillic hydrothermal alteration zones, whereas the pyrite + native sulphur veins are found within advanced argillic alteration zones. Fluid inclusion data indicate that the vein formation occurred at temperatures between about 125° and 370°C (sphalerite deposition formed at 123–211°C) from fluids with salinities of 0.5–4.6 wt. % eq. NaCl. Equilibrium thermodynamic interpretation of mineral assemblages indicates that the deposition of native sulphur in the upper and central portions of the hydrothermal system was a result of the mixing of condensates of ascending magmatic gases and meteoric water giving rise to fluids which had lower pH (<3.5) and higher fugacities of oxygen and sulphur than the lead-zinc-depositing fluids at depth. The $\delta^{34}S$ values of sulphide minerals from the lead-zinc veins ($\delta^{34}S$ = -4.6 to 0.7‰) are much higher than the values of pyrite and native sulphur from the pyrite + native sulphur veins ($\delta^{34}S$ = -12.9 to -20.1‰). This indicates that the fluids depositing native sulphur had higher sulphate/H_2S ratios under higher fo_2 conditions. Sulphur isotope compositions indicate an igneous source of sulphur with a $\delta^{34}S_{\Sigma S}$ value near 0‰, probably the Noel Hill Granodiorite. Measured and calculated $\delta^{18}O$ and δD values of the epithermal fluids ($\delta^{18}O_{water}$ = -6.0 to 2.7‰, δD_{water} = -87 to -75‰) indicate that local meteoric water played an important role for formation of lead-zinc and native sulphur-bearing quartz veins.

Received 4 January 1993, accepted 10 December 1994

Key words: Barton Peninsula, fossil hydrothermal system, mineral equilibria, geochemistry, Antarctica

Introduction

In the South Shetland Islands, a Jurassic-Quaternary island arc system located north of the Antarctic Peninsula, occurrences of "quartz-pyrite" rocks have been recognized and described by many workers (Ferguson 1921, Hawkes 1961, Barton 1964, Littlefair 1978, Park 1991). Barton (1964) described the quartz-pyrite rocks as mainly lodes of mineralized breccia that formed in shatter zones along pre-Tertiary faults. Littlefair (1978), however, proposed that they were irregular alteration zones derived from low-temperature epithermal-solfataric activity. Based on detailed mapping, Park (1991) developed a model for the alteration zoning and genesis of the epithermal system at the Barton Peninsula (*c.* 62°1'S longitude, 58°40'W latitude) on King George Island.

The present study aims to document the geochemistry and fluid evolution of the low-temperature, fossil hydrothermal system which was associated with explosive volcanism and subvolcanic intrusion in the Barton Peninsula, based on new fluid inclusion and stable isotope studies.

Description of epithermal system

The geology and geochronology of King George Island have been described by several authors (Hawkes 1961, Barton 1964, Davies 1982, Watts 1982, Smellie *et al.* 1984, Tokarski 1987, Kang & Jin 1988, Park 1989). The occurrence, mineralogy, and petrology of the epithermal quartz veins on the island were studied by Littlefair (1978) and Park (1991). In this section, we summarize the results of previous studies and report some new data.

General geology and wall-rock alteration

The South Shetland Islands represent a Jurassic-Quaternary island arc system where magmatic activity is thought to have moved progressively north-eastwards (Smellie *et al.* 1984). Barton Peninsula itself is composed mainly of volcanic and plutonic rocks. The volcanic rocks belong to the Fildes Formation (Barton 1964) and form a typical stratified volcanic-arc type succession. Based on different episodes of volcanic activity, the volcanic rocks are divided largely into two stratigraphical units (Tokarski 1987): lower and upper units (Fig. 1). The lower unit occurs along the southern margin of Barton Peninsula and is composed of red lapillistone and pyroclastic breccia. The upper unit which occupies much of the remainder of the peninsula is separated by an angular

https://doi.org/10.1017/S0954102095000101 Published online by Cambridge University Press

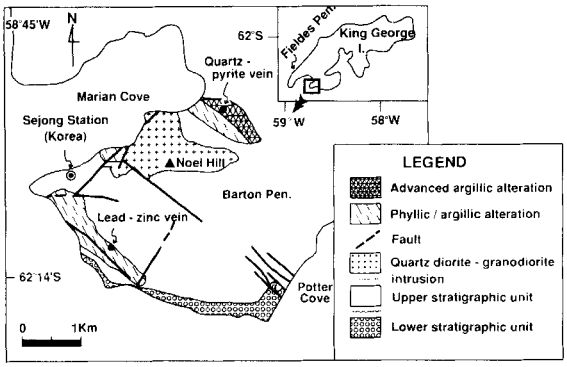

Fig. 1. A simplified geological map of Barton Peninsula (modified after Park 1991). Localities of hydrothermal alteration are also shown. Inset shows the position of the Barton Peninsula in the King George Island.

unconformity from the lower unit and is composed of green, black, and red andesitic lava flows, lapillistone, and pyroclastic breccia.

Volcanic rocks of the upper unit are intruded by a small plug, the Noel Hill Granodiorite, consisting mainly of fine- to medium-grained granodiorite and some quartz diorite (Fig. 1). A thermal metamorphic aureole surrounds the granodioritic plug (Littlefair 1978). Available K-Ar dates on the volcanic and plutonic rocks indicate an Eocene age (42–52 Ma) for the volcano-plutonic activity of Barton Peninsula (Watts 1982, Smellie *et al.* 1984, Park 1989).

Four types of wall-rock alteration were recognized and described by Littlefair (1978) and Park (1991): propylitic, phyllic (sericitic), argillic, and advanced argillic.

Propylitic alteration is most widespread, largely in linear zones especially around the Noel Hill Granodiorite, and is characterized by a quartz + epidote + sericite + chlorite + calcite ± pyrite assemblage. Quartz, epidote, pyrite, and minor amounts of pyrrhotite, chalcopyrite, rutile, and hematite (after magnetite) occur within veinlets in propylitic alteration zones. These chalcopyrite-bearing veinlets are thought to be an expression of the porphyry-copper system at depth (Littlefair 1978). Thus, the advanced argillic alteration at high altitudes of the Barton Peninsula may represent the superimposed phase on the top of the porphyry copper system formed around the Noel Hill Granodiorite (e.g. Sillitoe & Gappe 1984, Mitchell 1992).

The phyllic (sericitic) alteration occurs in linear zones along fault-related, fracture and breccia zones especially in the south-western part of the peninsula (Fig. 1). The alteration overprints the propylitic alteration and grades outward into the argillic alteration. The assemblage quartz + sericite + illite + calcite + pyrite ± kaolinite ± epidote ± chlorite is characteristic of the phyllic alteration.

The argillic alteration occurs around the phyllic alteration and is typified by the assemblage quartz + carbonates + pyrite + kaolinite ± dickite ± sericite ± rutile. Fine-grained pyrite and carbonates (calcite and dolomite) are abundant. Voids (<5 mm) in altered andesite, probably representing the sites of feldspar phenocrysts leached during the argillic alteration, are often filled with calcite and dolomite. Calcite veins are also abundant.

The advanced argillic alteration occurs at high altitudes in the northernmost parts of the peninsula (Fig. 1) and is characterized by a white, silica-rich groundmass in which lath-shaped voids are occasionally filled with native sulphur. Mineralogically the alteration consists of microcrystalline quartz, kaolinite, alunite (and minor natroalunite), pyrite, native sulphur, pyrophyllite, dickite, gypsum, barite and diaspore. The most strongly altered rocks occur centrally as quartz-rich, veins or irregular patches which contain pyrite, native sulphur, kaolinite, alunite and rutile.

Petrology and mineralogy of the quartz-pyrite rocks and lead-zinc veins

Quartz-pyrite rocks in the Barton Peninsula occur in advanced argillic alteration zones as disseminations, breccia pipes, and quartz veins and/or veinlets (Littlefair 1978, Park 1991). They usually occur along fault structures which formed during the explosive volcanism and intrusive activity (Park 1991). The quartz veins in advanced argillic alteration zones are often vuggy. Pyrite (<10 vol. %) usually forms mineralic bands at vein margins and is closely associated with fine-grained, anhedral to subhedral rutile. Native sulphur in the veins occurs as coarse grains near vugs and is occasionally associated with fine-grained pyrite and chalcedonic silica.

Sphalerite-galena-bearing quartz veins (each <5 cm thick) occur in the argillic alteration zones found in the south-west of the Barton Peninsula (Fig. 1) and were first described by Park (1991). The quartz is white to clear and often vuggy with platy crystal habits. Fine- to medium-grained, anhedral pyrites occur as disseminations in white quartz. Sphalerite and galena occur in clear quartz near or in vugs. Sphalerite is honey-coloured and often contains pyrite. Electron microprobe analysis of ten samples indicates that the sphalerite is very homogeneous in chemical composition and is exclusively iron-poor, containing FeS = 0.00–0.08 mole %, MnS = 0.00–0.06 mole %, and CdS = 0.14–0.28 mole %. A white-coloured, antimony-rich Cu-Sb(-As) mineral was observed within sphalerite during this study.

Distinct zoning of wall-rock alteration and ore mineralization is characteristic of volcanic-hosted epithermal systems (e.g. Buchanan 1981, Berger & Eimon 1983, Nuelle *et al.* 1985, Mitchell 1992). Quartz-alunite zones with native sulphur deposition typically occur in the upper (near-surface) and central parts of the system, whereas quartz-kaolinite-muscovite zones with base-metal deposition are usually found in the deeper and outer portions. Based on the general zoning pattern, the lead-zinc deposition and argillic alteration in the south-west of Barton Peninsula possibly represent the deeper and outer portions of the pyrite + native sulphur veins

and advanced argillic alteration at high levels in the northern part of the peninsula.

Fluid inclusion studies

Sixteen samples representing the two types of quartz veins of Barton Peninsula were selected for fluid inclusion studies (detailed sample descriptions are available from the authors upon request). Four to six doubly polished plates *c.* 1 mm thick were prepared for each sample and examined on a Fluid Inc. gas-flow-type heating-freezing stage at Korea University in order to obtain microthermometric data. The heating-freezing stage was calibrated with replicate measurements of microthermometric data of synthetic, H_2O- and CO_2-rich standard inclusions. Replicate measurements indicate that temperatures of homogenization and last ice-melting have standard errors of ±1.0°C and ±0.2°C, respectively.

The samples can be grouped into three types, according to locality and phase of alteration and hydrothermal activity: (1) white vein quartz, clear vug quartz, and honey-coloured sphalerite from lead-zinc-bearing quartz veins in argillic/phyllic alteration zones, (2) void-filling hydrothermal calcite in argillic-altered andesite, and (3) white vein quartz from pyrite and native sulphur-bearing quartz veins in advanced argillic alteration zones. Using the classification scheme of Roedder (1984), most inclusions examined appear to be primary in origin. Two hundred and fifty eight primary fluid inclusions were examined, in order to document ranges of fluid temperatures and compositions during the three types of mineralization. The cavity size of most inclusions is <50 μm in diameter (usually <15 μm).

Two types of inclusions are recognized from phase relations at room temperature: liquid-rich (type I) and vapour-rich (type II). Liquid-rich inclusions contain liquid and a small vapour bubble [determined by crushing and monitoring (during O-H isotope measurements) to be essentially water vapour] comprising <20% of the volume. These inclusions are dominant in all samples examined and homogenize to the liquid phase upon heating. They do not contain daughter minerals and no traces of gas hydrates were observed during freezing. Some vapour-rich inclusions occur within white quartz from lead-zinc and pyrite-native sulphur quartz veins. They contain liquid and a vapour bubble comprising 70–90% of the volume and apparently homogenize to the vapour on heating.

Salinity data are based on freezing-point depression in the system H_2O-NaCl (Potter *et al.* 1978). During the freezing experiments, the sequential cycling technique of Haynes (1985) was employed. Results of heating and freezing studies of fluid inclusions are presented in Figs 2, 3 & 4.

Heating and freezing data

Primary, liquid-rich inclusions in white vein quartz from lead-zinc-bearing quartz veins homogenize at temperatures

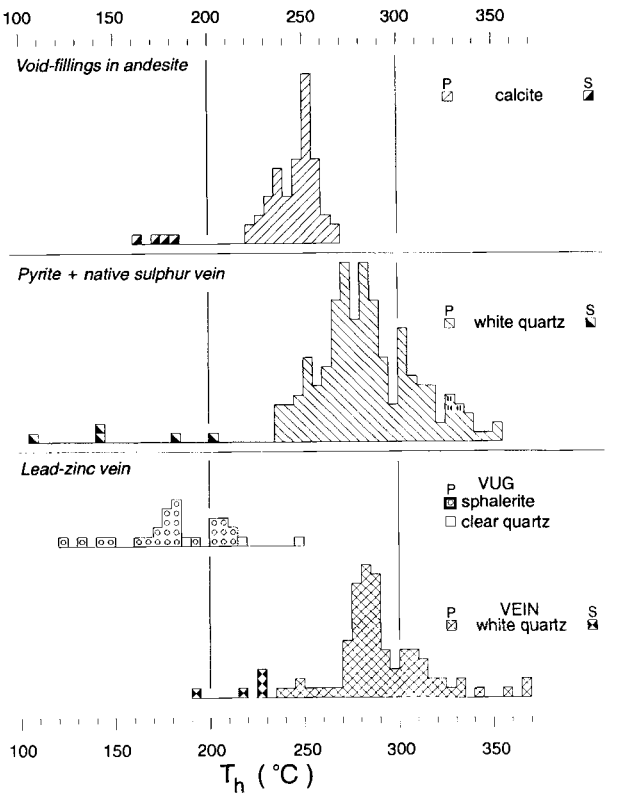

Fig. 2. Histograms of homogenization temperatures of fluid inclusions from epithermal quartz veins on Barton Peninsula. II = vapour-rich inclusions, P = primary, S = secondary.

of 239–369°C (mode at *c.* 280°C), whereas primary inclusions in clear quartz and sphalerite homogenize at the markedly lower temperatures of 188–247°C and 123–211°C, respectively (Fig. 2). Clear quartz was far from ideal for detailed fluid inclusion studies because of their inclusion rarity and, therefore, only three homogenization temperatures were obtained. Although some vapour-rich inclusions occur in white quartz, accurate homogenization temperatures could not be obtained due to the difficulty in observing the last remnants of liquid during heating (nevertheless, they seem to homogenize to a vapour in a temperature range of approximately 250–310°C). Measured salinities of primary, liquid-rich inclusions in minerals from the lead-zinc-bearing quartz veins are (Fig. 3): white vein quartz (0.7–2.9 wt. % eq. NaCl); sphalerite (2.9–4.6 wt. %).

Primary fluid inclusions in white quartz from pyrite and native sulphur-bearing quartz veins in advanced argillic alteration zones homogenize at temperatures of 236–350°C. Rare vapour-rich inclusions have homogenization temperatures of 326–334°C (Fig. 2). Salinities of fluid inclusions in the white quartz range from 0.9 to 3.7 wt. % eq. NaCl (Fig. 3). Chalcedonic quartz in vugs, which is often associated with coarse-grained native sulphur, was not suitable for study because of the absence of fluid inclusions.

Primary liquid-rich fluid inclusions in void-filling calcite from altered andesite homogenize at temperatures of

https://doi.org/10.1017/S0954102095000101 Published online by Cambridge University Press

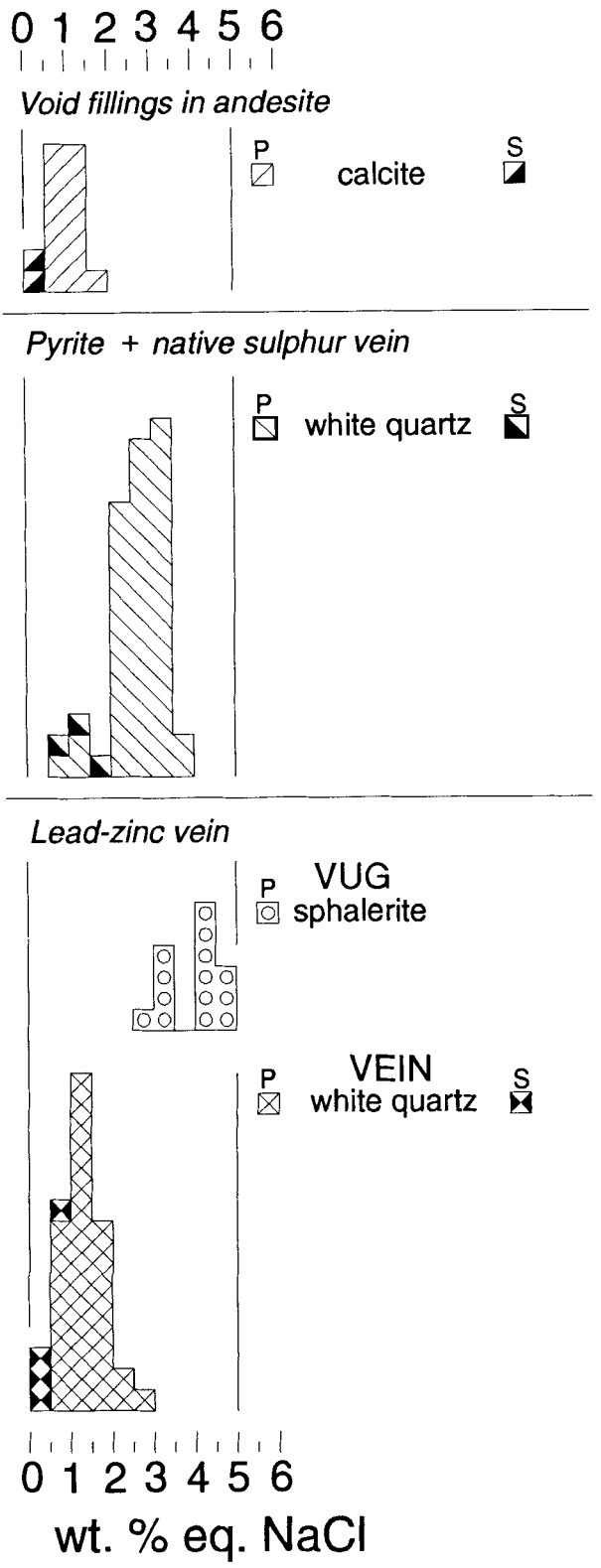

Fig. 3. Histograms of salinity data of fluid inclusions from epithermal quartz veins on Barton Peninsula. P = primary.

223–269°C (Fig. 2). They have salinities of 0.5–1.6 wt. % eq. NaCl (Fig. 3).

Variations in temperature and composition of epithermal fluids

The relationship between homogenization temperature and salinity of fluid inclusions (Fig. 4) indicates a complex history of boiling, cooling, and dilution of the fossil epithermal fluids on Barton Peninsula. Decreasing salinity with decreasing temperature for the fluids from which white vein quartz in the lead-zinc-bearing quartz veins was deposited probably indicates the cooling and dilution of the fluids by mixing with less-evolved meteoric waters (Fig. 4). Progressive downward introduction of cooler dilute meteoric waters into the hydrothermal system possibly resulted in the deposition of void-filling calcite in altered andesite.

Salinities of the fluids from which honey-coloured sphalerite near or in vugs was deposited are higher than those of earlier, white quartz-depositing fluids, whereas the temperatures are much lower (Fig. 4). Two possible explanations for this phenomenon are: (1) later, boiling and vapour loss of hydrothermal fluids, resulting in an increase of salinity (up to 4.6 wt. % eq. NaCl) with cooling, or (2) later mixing of hydrothermal fluids with more saline (>4.5 wt. % eq. NaCl) and cooler fluids. Case (1) is preferred because the association of some vapour-rich fluid inclusions with liquid-rich inclusions in white quartz from lead-zinc-bearing quartz veins may evidence the fluid boiling. The correspondence between homogenization temperatures of fluid inclusions in sphalerite and temperatures determined from sulphur isotope fractionations (175–202°C) further indicates that fluid pressure was close to the vapour saturation.

For fluid inclusions in white quartz from the pyrite and native sulphur-bearing quartz veins, there is no clear relationship between homogenization temperature and salinity (Fig. 4). Salinities of the fluids responsible for the deposition of pyrite and native sulphur are higher than those of the hydrothermal fluids associated with deposition of white quartz in lead-zinc-bearing quartz veins, and are lower than those of the fluids responsible for the deposition of sphalerite. These phenomena are interpreted to indicate that the fluids for pyrite and native sulphur deposition in advanced argillic alteration zones represent a condensate of more saline (>3 wt. % NaCl), lead-zinc-deposited fluids which were increased in salinity through boiling.

Geochemical environments

Equilibrium thermodynamics were used to estimate the geochemical conditions of the epithermal fluids at Barton Peninsula. Although a number of assumptions were used to estimate the conditions, the evaluation of parameters (fs_2, fo_2, pH, etc.) would be helpful to compare qualitatively the lead-zinc and the pyrite + native sulphur deposition and

https://doi.org/10.1017/S0954102095000101 Published online by Cambridge University Press

to understand the evolution of an epithermal system formed at Barton Peninsula.

Sulphur fugacity

Fluid inclusion and sulphur isotope data indicate that sphalerite in lead-zinc-bearing quartz veins was deposited from boiled fluids at temperatures between ~120° and 210°C. The probable ranges of sulphur fugacity (fs_2) for the sphalerite deposition can be estimated from the phase relations in the system Fe-Zn-S (Barton & Toulmin 1966, Barton & Skinner 1979) and the equilibrium assemblage pyrite + sphalerite (mole % FeS = 0.00–0.08). The estimated log fs_2 values for the deposition of sphalerite range from about -18 to -12 atm at ~120–210°C.

Due to the absence of fluid inclusions in chalcedonic quartz associated with native sulphur in pyrite + native sulphur veins, the temperature conditions for native sulphur deposition could not be estimated. Based on the paragenetic constraint that native sulphur was deposited later than white vein quartz, however, depositional temperatures of native sulphur can be assumed to be less than 235°C (the lower limit of homogenization temperatures of fluid inclusions in white vein quartz, Fig. 2). In addition, the mineral assemblage quartz + kaolinite + pyrophyllite + diaspore in the advanced argillic alteration zones around the native sulphur-bearing quartz veins suggests that temperatures were below 285° ± 10°C under the liquid-vapour coexistence conditions (Hemley *et al.* 1980). At temperatures of <150–235°C, sulphur condensation occurs at log fs_2 values of about -8 to -5 atm to form native sulphur (Barton & Skinner 1979). The fairly high sulphur fugacities for the native sulphur deposition and advanced argillic alteration may indicate a significant contribution of sulphur-rich magmatic gases to the fluids, as suggested by Stoffregen (1985) for the Summitville district, Colorado.

Oxygen fugacity

Fugacity of oxygen can be estimated from the stability relations of characteristic mineral assemblages. Probable fs_2–fo_2 fields were constructed at 200°C in order to compare conditions responsible for lead-zinc and pyrite + native sulphur deposition (Fig. 5).

Neither liquid CO_2 nor CO_2 hydrate were observed to nucleate on cooling of fluid inclusions. Combined with the monitored compositions of the fluids extracted for the O-H isotope analysis, these data indicate that molar proportion of CO_2 (Xco_2) is negligible (likely <0.0005) in the epithermal fluids at Barton Peninsula. Fluid inclusions indicate that fluid salinities were usually less than 0.5 molal at 200°C. Values of fco_2 for the fluids can be constrained by utilizing Henry's law ($K = fco_2/Xco_2$). Henry's law constant (K) for a 0.5 molal NaCl solutions at 200°C is 6,800 (Ellis & Golding 1963). Calculation yields an upper limit of log fco_2 value of

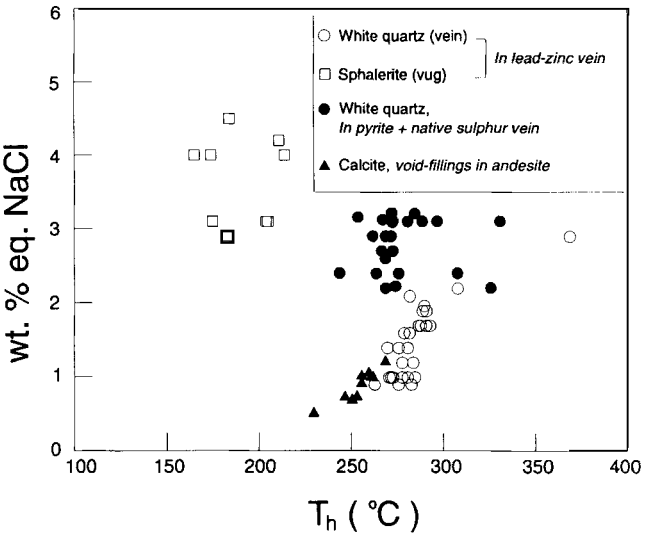

Fig. 4. Homogenization temperature versus salinity diagram for fluid inclusions from epithermal quartz veins on Barton Peninsula.

0.53 at 200°C. Thus, a maximum log fco_2 value of 0.6 was used for the calculations of C-CO_2 and $CaCO_3$-$CaSO_4$ equilibria.

Based on the estimated log fs_2 value (-12.3 atm at 200°C) for the sphalerite (<0.08 mole % FeS) + pyrite deposition (Barton & Toulmin 1966) and the absence of graphite in lead-zinc veins, the probable log fo_2 (atm) values for sphalerite deposition at 200°C are estimated to be about -43 to -37.5 (hatched area in Fig. 5).

Probable fo_2 conditions for native sulphur deposition can be set by the kaolinite-alunite (-gypsum) equilibria (Hemley *et al.* 1969, Helgeson 1969) and the estimated log fs_2 value (-5.5 atm at 200°C) for sulphur condensation (Barton & Skinner 1979). For the calculation of kaolinite-alunite equilibria, the molality of K^+ was estimated to be about 0.03 molal at 200°C, based on the estimated salinities (average 0.5 molal solutes) and the empirical and theoretical curves between temperature and Na/K atomic ratio for geothermal waters (Fournier & Truesdell 1973). This approach is based on the assumption that K-Na-aluminosilicate-bearing assemblages in rocks were in complete equilibrium with the hydrothermal fluids. The pH of the fluids was assumed to fall in the approximate range of 2.5 to 4.0 because the kaolinite + alunite assemblage is stable under acidic conditions. The estimated log fo_2 values for native sulphur deposition are -38.0 ± 0.5 atm at 200°C (dotted area in Fig. 5). Assuming that HSO_4^- was the dominant sulphur species in native sulphur-deposition fluids, total sulphur concentrations (mεS) in the fluids can be calculated using the reaction $HSO_4^- + H^+ = 3/2O_2 + 1/2S_2 + H_2O$ (Helgeson 1969, Helgeson *et al.* 1978) and the activity coefficients determined according to the method described in Helgeson (1969). Using the estimated fo_2, fs_2 and pH conditions at 200°C for the pyrite + native sulphur deposition (Fig. 5), the probable range of mεS

https://doi.org/10.1017/S0954102095000101 Published online by Cambridge University Press

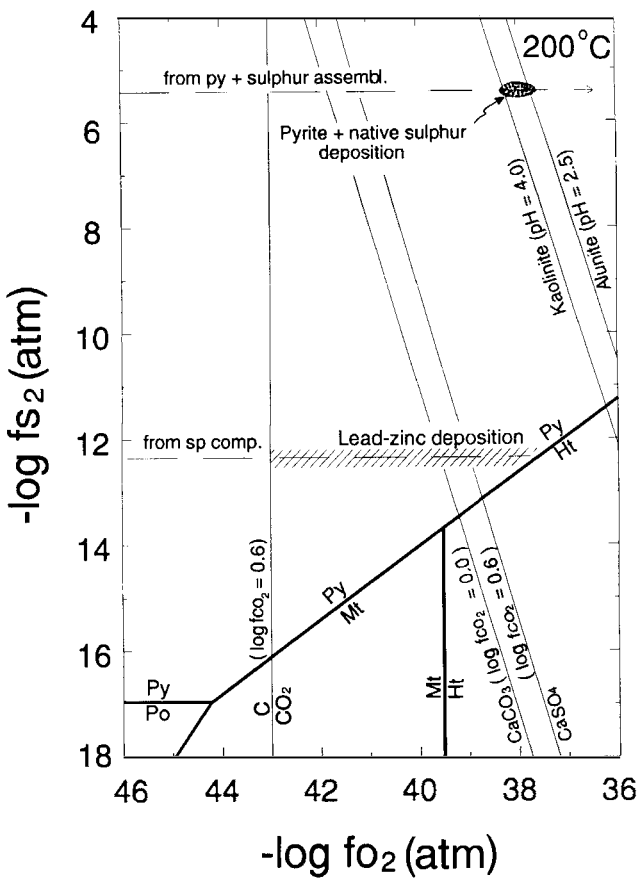

Fig. 5. An isothermal log fs_2 versus log fo_2 diagram showing the mineral stability fields for the significant minerals at 200°C. The hatched area and the dotted area show the most likely environments for the lead-zinc deposition and the pyrite + native sulphur deposition, respectively. Thick solid lines = boundaries between pyrite (Py), pyrrhotite (Po), magnetite (Mt), and hematite (Ht) (Barton & Skinner 1979); Horizontal dashed lines = the fs_2 conditions calculated from the iron content of sphalerite (Barton & Toulmin 1966) and the stability of pyrite + native sulphur assemblage (Barton & Skinner 1979); Oblique light solid lines = the stability boundaries between calcite and gypsum at different log fco_2 conditions (Robie *et al.* 1978) and the boundaries between kaolinite and alunite plus quartz at different pH conditions for a 0.5-molal saline solution with Na/K = 15 (Hemley *et al.* 1969).

values is calculated to be $10^{-2.5}$ to $10^{-2.0}$. This mεS range is similar to the range for many epithermal veins (10^{-2} to 10^{-3}) based on thermodynamic calculations and chemical analysis of base-metal-depositing hot springs (e.g. Browne 1971, Shikazono 1972).

pH and geochemical evolution

The pH values of hydrothermal fluids can be determined using the stability relations of alteration minerals (Helgeson 1969, Hemley *et al.* 1969). Kaolinite and minor amounts of sericite occur as typical alteration minerals in argillic alteration zones around the lead-zinc veins, whereas kaolinite and alunite are found in advanced argillic alteration zones around the pyrite + native sulphur veins. At a molality of potassium ion (mK^+) of about 0.03, kaolinite coexists with muscovite at a pH of about 5.5 and with alunite at a maximum pH of about 3.4.

The likely fo_2–pH environments at 200°C for epithermal fluids can be defined using calculated $\delta^{34}S$ values of H_2S in fluids (Fig. 6). For the calculation of $\delta^{34}S_{H_2S}$ contours, the $\delta^{34}S_{\Sigma S}$ value was assumed to be 0‰ (see "Stable isotope studies"). The deposition of sphalerite in lead-zinc veins probably occurred from slightly acidic fluids with log fo_2 of ≈-42 to -39 atm and pH of ≈-3.5 to -5.5 (hatched area in Fig. 6), whereas native sulphur in pyrite + native sulphur veins deposited from more oxidizing, acidic fluids with log fo_2 of ≈-39 to -36 atm and pH of ≈1 to 3.5 (dotted area in Fig. 6). These estimated fo_2 conditions generally fit with the conditions from Fig. 5.

Calculations of geochemical parameters indicate that the pyrite + native sulphur deposition and advanced argillic alteration at Barton Peninsula formed from fluids which are characterized by higher acidity (pH<3.5) and higher fugacities of oxygen and sulphur than the fluids responsible for lead-zinc veins. These characteristics are similar to those reported for worldwide, volcanic-hosted epithermal systems (e.g. Mitchell 1992), where the "acid-sulphate" fluids are produced by interaction between a large mass of SO_2-rich, magmatic gas and deeply circulating, meteoric water.

Stable isotope studies

Stable isotope data can be used to elucidate the origin and history of epithermal fluids. In this study the sulphur isotope compositions of eight sulphides and two native sulphurs, the carbon and oxygen isotope compositions of two calcites and seven quartzes, and the hydrogen isotope compositions of inclusion waters from four quartzes were measured. Standard techniques of extraction and analysis were used (McCrea 1950, Grinenko 1962, Hall & Friedman 1963, Rye 1966). The analyses were performed using a Finnigan MAT Delta E gas-source mass spectrometer in the University of Missouri-Columbia. Data are reported in standard δ notation relative to the CDT standard for S, the PDB standard for C, and the Vienna SMOW standard for O and H. The standard error for each analysis is approximately ±0.1‰ for S, C, and O, and ±2‰ for H isotopes.

Sulphur isotope study

Sulphur isotope data are summarized in Table I. The $\delta^{34}S$ values of minerals range widely from -20.1 to 0.7‰. Sulphide minerals from the lead-zinc quartz veins in argillic alteration zones have $\delta^{34}S$ values of -4.6 to 0.7‰. On the other hand, the $\delta^{34}S$ values of pyrite and native sulphur from the pyrite +

https://doi.org/10.1017/S0954102095000101 Published online by Cambridge University Press

native sulphur veins in the advanced argillic alteration zones are remarkably low, ranging from -20.1 to -12.9‰.

Two sphalerite-galena pairs with equilibrium textures from lead-zinc veins have $\Delta^{34}S$ values of 3.2 and 3.6‰, yielding equilibrium isotope temperatures of 202 ± 29°C and 175 ± 27°C (Ohmoto & Rye 1979) (Table I). These sulphur isotope temperatures are in good agreement with homogenization temperatures (123–211°C, Fig. 2) of primary fluid inclusions in sphalerite which occurs near or in vugs.

Based on sulphur isotope temperatures, $\delta^{34}S$ values of sulphur species in the hydrothermal fluids can be calculated from compiled equations in Ohmoto & Rye (1979). The probable ranges of $\delta^{34}S$ values for H_2S and SO_4^{2-} for lead-zinc deposition are -5.1 to 0.2‰ and 27.1 to 32.4‰, respectively. The sulphur isotope composition of the entire solution ($\delta^{34}S_{\Sigma S}$) depends on the molar ratio between H_2S and sulphates in solution: the lower the H_2S/sulphate ratio under higher fo_2 conditions, the higher the $\delta^{34}S_{\Sigma S}$ value. Assuming that H_2S was the dominant sulphur species in the lead-zinc depositing fluids (Fig. 6), $\delta^{34}S_{H_2S}$ values may be taken as an approximation of $\delta^{34}S_{\Sigma S}$ values. The near 0‰ $\delta^{34}S_{\Sigma S}$ value for the lead-zinc deposition may indicate an igneous source of sulphur (Ohmoto & Rye 1979, Hoefs 1980).

The $\delta^{34}S$ values of pyrite from the pyrite + native sulphur veins phase are -20.1 to -14.6‰ (including two pyrites from alteration zones adjacent to veins, -20.1 to -17.1‰). Pyrite in the pyrite + native sulphur veins occurs as an early-deposited mineral forming marginal bands. Assuming depositional temperatures of 300–350°C for these pyrites [based on a high-temperature cluster within the wide range of homogenization temperatures of fluid inclusions in white quartz (Fig. 2), assuming that the fluid temperatures lowered progressively with time], calculated $\delta^{34}S$ values of H_2S and SO_4^{2-} during the pyrite deposition are -21.1 to -15.8‰ and -12.8 ± 0.5 to -7.1 ± 0.5‰, respectively (Ohmoto & Rye 1979). It is noteworthy that there is an at least -11‰ difference in calculated $\delta^{34}S_{H_2S}$ values between the lead-zinc deposition (-5.1 to 0.2‰) and the pyrite deposition. This may reflect chemically and isotopically different evolution of sulphur reservoirs for the two types of mineral precipitation. Lower $\delta^{34}S_{H_2S}$ values for the pyrite deposition also can be explained by the higher oxidation state of the fluids and, therefore, the lower H_2S/sulphate ratio (Figs 5 & 6) because sulphates are stable under oxidizing conditions and preferentially incorporate ^{34}S to cause residual H_2S to become isotopically lighter (Ohmoto 1972, Ohmoto & Rye 1979). Such higher oxidation state of the fluids responsible for the pyrite deposition and acid-sulphate alteration could have

Table I. Sulphur isotope data from a fossil epithermal system at Barton Peninsula.

Deposition phase	Sample no.	Mineral	$\delta^{34}S$ (‰)	$\Delta^{34}S_{sp-gn}$ (‰)	T (°C)[1]	Comments
Lead-zinc	P2-2	sphalerite	-4.6			L
	P2-3	sphalerite	0.7			
				3.6	175 ± 27	
		galena	-2.9			L
	P3	sphalerite	0.5			
				3.2	202 ± 29	
		galena	-2.7			L
Pyrite + native sulphur	S4	pyrite	-20.1			E, A
	157-1	pyrite	-17.1			E, A
	157-2	pyrite	-14.6			E
	157-3	native sulphur	-12.9			L
		native sulphur	-13.3			L

[1] Using compiled isotope fractionation factors of Ohmoto & Rye (1979).
Abbreviations: A = in alteration zones; E = early; L = late (in or near vugs).

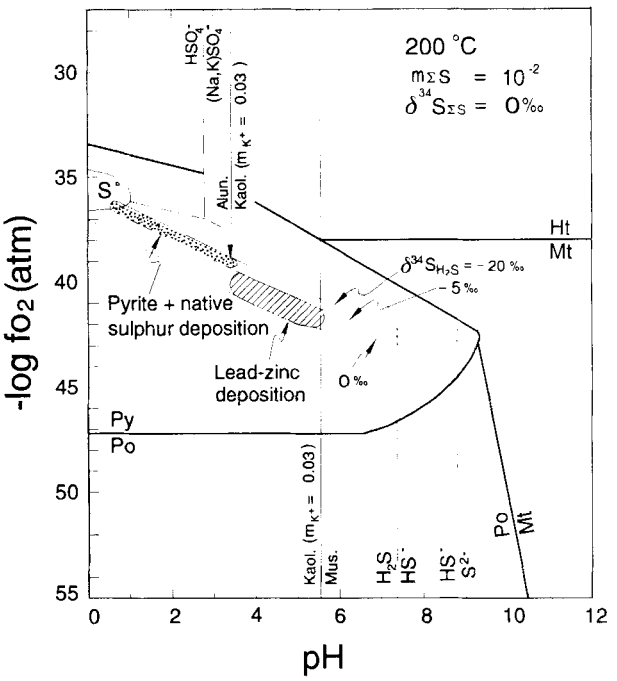

Fig. 6. An isothermal log fo_2 versus pH diagram showing the stability relations of the significant minerals and the sulphur isotope compositions of H_2S at 200°C, $m\Sigma S = 10^{-2}$ molal, and $\delta^{34}S_{\Sigma S} = 0$‰. The hatched area and the dotted area show the most likely environments for the lead-zinc deposition and the pyrite + native sulphur deposition, respectively. Thick solid lines = mineral stability boundaries between pyrite (Py), pyrrhotite (Po), magnetite (Mt), and hematite (Ht) [calculated from Helgeson (1969), except the equilibrium constant from Ohmoto (1972) for pyrite-pyrrhotite reaction]; Dashed lines = equal molality boundaries between aqueous sulphur species (Helgeson 1969); Vertical light solid lines = Stability boundaries between kaolinite and muscovite (Helgeson 1969) and between alunite and kaolinite (Hemley *et al.* 1969) at $m_{K+} = 0.03$; Light solid curves = $\delta^{34}S$ contours for H_2S under a condition of $\delta^{34}S_{\Sigma S} = 0$‰ (calculated using the method in Ohmoto, 1972).

https://doi.org/10.1017/S0954102095000101 Published online by Cambridge University Press

Table II. Carbon, oxygen, and hydrogen isotope data for quartz, calcite, and their inclusion waters from epithermal quartz veins at Barton Peninsula.

Deposition phase	Sample no.	Mineral	$\delta^{13}C$ (‰)	$\delta^{18}O$ (‰)	T (°C)[1]	$\delta^{18}O_{water}$ (‰)[2]	δD (‰)	Comments
Lead-zinc	P1	white quartz		5.3	300	-1.6	-83	E
	P2-1	white quartz		4.5	310	-2.0	-87	E
	P2-3	clear quartz		7.3	175	-6.0		L
	P3-1	white quartz		8.4	280	0.8	-75	M
	155	white quartz		3.3	280	-4.3	-78	M
Pyrite + native sulphur	S5	white quartz		6.2	300	-0.7		E
	157	white quartz		4.3	280	-3.3		M
Carbonate	38	void-filling calcite in andesite	-4.2	9.9	250	2.7		
	94	calcite in veins	-5.0	10.9				

[1]Based on homogenization temperatures for fluid inclusions in the same samples and paragenetic constraints. Temperature variations of approximately ± 20°C would result in deviations of approximately ± 0.5 and ± 0.9‰ in calculated $\delta^{18}O_{water}$ values for quartz and calcite, respectively.
[2]Calculated water compositions based on quartz-water and calcite-water oxygen isotope fractionations of Matsuhisa *et al.* (1979) and O'Neil *et al.* (1969), respectively. Abbreviations: E = early; M = middle; L = late (in or near vugs).

resulted from the condensation of ascending, vapour phase-rich boiling fluids into an overlying, more oxidizing ground water system (Cunningham *et al.* 1984, Rye *et al.* 1989).

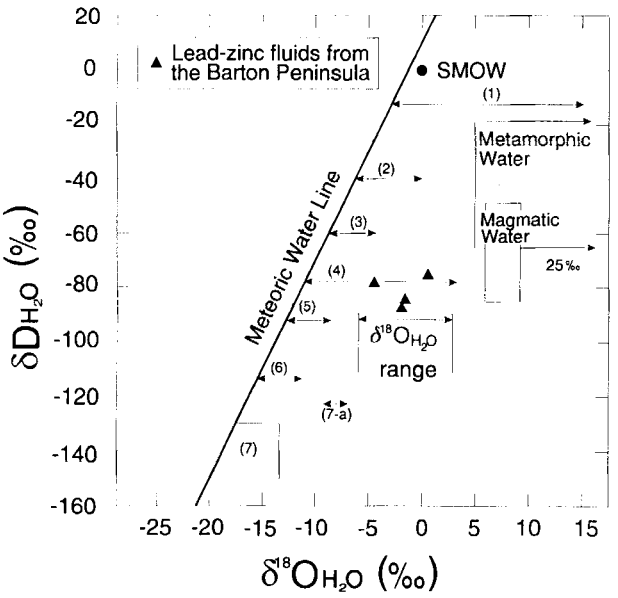

Fig. 7. Hydrogen versus oxygen isotope diagram showing hydrothermal fluid compositions for a fossil epithermal system at Barton Peninsula (black triangles). Calculated range of $\delta^{18}O_{water}$ values are also shown. The magmatic and metamorphic water boxes are from Taylor (1974); the meteoric water line is from Craig (1961). Numbered horizontal lines and box represent the oxygen and hydrogen isotope compositions of hot spring, fumarole, and drill hole thermal waters from a number of well-known modern geothermal systems (Truesdell & Hulston 1980): 1 = Lanzarote; 2 = Wairakei/Broadlands and Larderello; 3 = The Geysers; 4 = Salton Sea; 5 = Lassen Peak; 6 = Steamboat Springs; 7 = Yellowstone Park (7-a from acid springs).

Assuming that native sulphur deposited at temperatures between 150° and 235°C, the probable ranges of $\delta^{34}S$ values for H_2S and SO_4^{2-} are calculated to be -12.7 ± 0.5 to -12.0 ± 0.5‰ and -5.2 ± 1.0 to -3.0 ± 1.0‰, respectively (Ohmoto & Rye 1979). The calculated $\delta^{34}S$ values of sulphates in solution during native sulphur deposition are near to the $\delta^{34}S$ value of H_2S (-5.1 to 0.2‰) during lead-zinc deposition. This also may indicate that the molar proportion of dissolved sulphates relative to H_2S in solution was much higher during native sulphur deposition than lead-zinc deposition.

Within the pyrite + native sulphur deposition there is an apparent increase in $\delta^{34}S$ values of H_2S with time: early pyrite, -21.1 to -15.8‰; and late native sulphur, -12.7 to -12.0‰. Three possible explanations for this phenomenon are: (1) gradual addition of sulphur from an isotopically heavy source (possibly sulphates from volcano-sedimentary wall rocks and/or sea water); (2) an original isotopically heavy sulphur source (at least -12‰) with an increasing H_2S/sulphate ratio (reduction of sulphur); (3) isotopic reequilibration in the fluid following removal of H_2S by boiling or precipitation of pyrite (reservoir effect). Case (1) seems unlikely because $\delta^{18}O$ and δD data for epithermal fluids at Barton Peninsula indicate the dominance of local meteoric waters in the hydrothermal system. Case (2) also seems unlikely because mineralogical data indicated oxidation with time. Explanation (3) is therefore preferred. Drummond & Ohmoto (1985) have shown that with boiling and condensation of hydrothermal fluids, significant changes in molar ratio H_2S/sulphate occur. Continued, boiling, vapour-phase ascent and condensation under near-surface conditions would result also in preferential loss of ^{32}S-rich H_2S and higher $\delta^{34}S$ values of residual H_2S and S-bearing minerals. This increase in the $\delta^{34}S_{H_2S}$ value for pyrite + native sulphur deposition, therefore, may support the notion that the pyrite + native sulphur depositing fluid represent the condensates of gaseous components from ascending boiling fluids.

https://doi.org/10.1017/S0954102095000101 Published online by Cambridge University Press

Carbon, oxygen and hydrogen isotope studies

One void-filling calcite in altered andesite and one calcite from a vein have $\delta^{13}C$ values of -4.2‰ and -5.0‰, respectively (Table II). These $\delta^{13}C$ values fall within the range of $\delta^{13}C$ data (-10 to 1‰) for most geothermal systems and epithermal deposits (Field & Fifarek 1986). Assuming that these calcites were deposited at temperatures between 150° and 250°C (based on homogenization temperatures of fluid inclusions, Fig. 2), the probable range of $\delta^{13}C$ values for H_2CO_3 in hydrothermal fluids is calculated to be -2.9 to -6.5‰ [using the isotope fractionation equation of Bottinga (1969)].

The $\delta^{18}O$ values of seven quartz samples are: lead-zinc veins, 3.3 to 8.4‰; pyrite + native sulphur veins, 4.3 to 6.2‰ (Table II). Using the quartz-water fractionation equation of Matsuhisa *et al.* (1979) coupled with paragentic constraints and homogenization temperatures for fluid inclusions from the same samples, calculated $\delta^{18}O$ values of water are (Table II): lead-zinc deposition, -6.0 to 0.8‰; pyrite + native sulphur deposition, -3.3 to -0.7‰.

The $\delta^{18}O$ values of calcite samples are: one void-filling calcite in andesite, 9.9‰; one vein calcite, 10.9‰ (Table II). Using the calcite-water isotope fractionation equation of O'Neil *et al.* (1969) coupled with mean homogenization temperatures for fluid inclusions, the $\delta^{18}O$ value of water in equilibrium with the void-filling calcite is calculated to be 2.7‰ (Table II). Assuming that vein calcites from argillic alteration zones were deposited at temperatures of 150–250°C, the probable range of $\delta^{18}O_{water}$ values is -2.1 to 3.7‰.

Inclusion waters were extracted from four white quartz samples from lead-zinc veins and were measured for hydrogen isotope compositions. Special care was taken to select samples for analysis that contain a high proportion of primary fluid inclusions. Other samples were not suitable for study due to the difficulty of collection of large quantities of mineral separates. The δD values of inclusion waters from lead-zinc veins range from -87 to -75‰ (Table II).

Interpretation of O-H isotope results

Measured and calculated hydrothermal fluid compositions from the fossil epithermal systems on Barton Peninsula are shown on a conventional H versus O isotope diagram (black triangles in Fig. 7). For comparison, compositional variations of subsurface waters associated with a number of well-known geothermal systems (Truesdell & Hulston 1980) are also shown. The "oxygen isotope shift" caused by isotope exchange reactions between ^{18}O-depleted meteoric waters and ^{18}O-enriched rocks during water-rock interaction (Taylor 1974) is common in the subsurface fluids of many geothermal systems. The size of the ^{18}O-shift correlates directly with temperature and salinity of the fluids, and inversely with water/rock mass ratios. The slight positive shift in δD values for the Yellowstone geothermal area was interpreted as a result of boiling and condensation of subsurface waters (Truesdell *et al.* 1977). Thus, the distribution of $\delta^{18}O$ and δD values for modern geothermal fluids records their meteoric source.

The range of data for lead-zinc-bearing quartz veins on Barton Peninsula is also consistent with a meteoric water source and is similar to that for subsurface waters from the geothermal system at Salton Sea (Fig. 7). The fluids associated with lead-zinc veins at Barton Peninsula could have resulted from exchange reactions between local meteoric water (without any contribution of sea water) and nearly equal amounts of rock. Although the δD_{water} values for pyrite + native sulphur deposition were not measured, the $\delta^{18}O_{water}$ values (3.3 to -0.7‰, Table II) being much lower than the $\delta^{18}O$ range of primary magmatic waters (5.5–10‰, Taylor 1974) indicate that the "acid-sulphate waters" (Heald *et al.* 1987) responsible for the formation of pyrite + native sulphur veins and advanced argillic alteration probably were dominated by the meteoric water of appropriate composition. There are few available $\delta^{18}O$–δD data for hydrothermal fluids from "acid-sulphate-type" deposits but Taylor (1973) suggested that for the "acid-sulphate-type" deposits in the Goldfield district, Nevada, the water in hydrothermal fluids was essentially 100% of meteoric origin.

Acknowledgements

This research was supported financially by a grant from the Center for Mineral Resources Research (CMR) sponsored by the Korea Science and Engineering Foundation. We thank Drs J.A. Plant and J. Ridgway (British Geological Survey) for their constructive comments on the manuscript. The paper was greatly improved by comments from Dr M.R.A. Thomson and two anonymous reviewers.

References

Barton, C.M. 1964. The geology of the South Shetland Islands: III. The stratigraphy of King George Island. *British Antarctic Survey Scientific Reports*, No. 44, 33pp.

Barton, P.B., Jr. & Skinner, B.J. 1979. Sulfide mineral stabilities. *In* Barnes, H.L. *ed. Geochemistry of hydrothermal ore deposits*. New York: Wiley and Sons Pub. Co., 278-408.

Barton, P.B., Jr. & Toulmin, P., III. 1966. Phase relations involving sphalerite in the Fe-Zn-S system. *Economic Geology*, **61**, 815-849.

Berger, B.R. & Eimon, P.I. 1983. Conceptual models of epithermal precious metal deposits. *In* Shanks, W.C. *ed. Cameron volume on unconventional mineral deposits*. New York: Society of Mining Engineers, 191-205.

Bottinga, Y. 1969. Calculated fractionation factors for carbon and hydrogen isotope exchange in the system calcite-carbon dioxide-graphite-methane-hydrogen-water vapor. *Geochimica et Cosmochimica Acta*, **33**, 49-64.

Browne, P.R.L. 1971. Mineralization in the Broadland geothermal field, Taupo volcanic zone, New Zealand. *Society of Mining Geologists Japan Special Issue* No. 2, 64-75.

Buchanan, L.J. 1981. Precious metal deposits associated with volcanic environments in the southwest. *In* Dickinson, W.R. & Payne, W.D. *eds.* Relations of tectonics to ore deposits in the South Cordillera. *Arizona Geological Society Digest*, **XIV**, 237-261.

Craig, H. 1961. Isotopic variations in meteoric waters. *Science*, **133**, 1702-1703.

Cunningham, C.G., Rye, R.O., Steven, T.A. & Mehnert, H.H. 1984. Origins and exploration significance of replacement and vein-type alunite deposits in the Marysvale volcanic field, west central Utah. *Economic Geology*, **79**, 50-71.

Davies, R.E.S. 1982. The geology of the Marian Cove area, King George Island, and a Tertiary age for its supposed Jurassic volcanic rocks. *British Antarctic Survey Bulletin*, No. 51, 151-165.

Drummond, S.E. & Ohmoto, H. 1985. Chemical evolution and mineral deposition in boiling hydrothermal systems. *Economic Geology*, **80**, 126-147.

Ellis, A.J. & Golding, R.M. 1963. The soubility of carbon dioxide above 100°C in water and in sodium chloride solutions. *American Journal of Science*, **261**, 47-60.

Ferguson, D. 1921. Geological observations in the South Shetlands, Palmer Archipelago, and Graham Land, Antarctica. *Royal Society of Edinburgh, Transaction*, No. 53, pt. 1, 29-55.

Field, C.W. & Fifarek, R.H. 1986. Geology and geochemistry of epithermal systems: Light stable-isotope systematics in the epithermal environment. *In* Berger, B.R. & Bethka, P.M. *eds. Reviews in Economic Geology*, **2**, 99-128.

Fournier, R.O. & Truesdell, A.H. 1973. An empirical Na-K-Ca geothermometer for natural waters. *Geochimica et Cosmochimica Acta*, **37**, 1255-1275.

Grinenko, V.A. 1962. Preparation of sulfur dioxide for isotopic analysis. *Zeitschrift Neorganische Khimii*, **7**, 2478-2483.

Hall, W.E. & Friedman, I. 1963. Composition of fluid inclusions, Cave-in-Rock fluorite district, Illinois and Upper Mississippi Valley zinc-lead district. *Economic Geology*, **58**, 886-911.

Haynes, F.M. 1985. Determination of fluid inclusion compositions by sequential freezing. *Economic Geology*, **80**, 1436-1439.

Hawkes, D.D. 1961. The geology of the South Shetland Islands : 1. The petrology of King George Island. *Falkland Islands Dependencies Survey Scientific Reports*, No. 26, 28pp.

Heald, P., Foley, N.K. & Hayba, D.O. 1987. Comparative anatomy of volcanic-hosted epithermal deposits: Acid-sulfate and adularia-sericite types. *Economic Geology*, **82**, 1-26.

Helgeson, H.C. 1969. Thermodynamics of hydrothermal systems at elevated temperatures and pressures. *American Journal of Science*, **267**, 729-804.

Helgeson, H.C., Delany, J.M., Nesbitt, H.W. & Bird, D.K. 1978. Summary and critique of the thermodynamic properties of rock-forming minerals. *American Journal of Science*, **278-1**, 1-229.

Hemley, J.J., Hostetler, P.B., Gude, A.J. & Mountjoy, W.T. 1969. Some stability relations of alunite. *Economic Geology*, **64**, 599-612.

Hemley, J.J., Montoya, J.W., Marinenko, J.W. & Luce, R.W. 1980. Equilibria in the system Al_2O_3-SiO_2-H_2O and some general implications for alteration/mineralization process. *Economic Geology*, **75**, 210-228.

Hoefs, J. 1980. *Stable isotope geochemisty*. 2nd ed. Berlin-Heidelberg: Springer-Verlag, 208pp.

Kang, P.C. & Jin, M.S. 1988. Petrology and geologic structures of the Barton Peninsula, King George Island, Antarctica. *In* Huh, *et al. eds. Antarctic Science: Geology and biology*. Seoul: Korea Ocean Research and Development Institute, 121-135. [In Korean.]

Littlefair, M.J. 1978. The "quartz-pyrite" rocks of the South Shetland Islands, Western Antarctic Peninsula. *Economic Geology*, **73**, 1184-1189.

Matsuhisa, Y., Goldsmith, R. & Clayton, R.N. 1979. Oxygen isotope fractionation in the system quartz-albite-anorthite-water. *Geochimica et Cosmochimica Acta*, **43**, 1131-1140.

McCrea, J.M. 1950. The isotope chemistry of carbonates and a paleotemperature scale. *Journal of Chemical Physics*, **18**, 849-857.

Mitchell, A.H.G. 1992. Andesitic arcs, epithermal gold and porphyry-type mineralization in the western Pacific and eastern Europe. *Transactions of the Institution of Mining and Metallurgy (Section B: Applied Earth Sciences)*, **101**, B125-B138.

Nuelle, L.M., Proctor, P.D. & Grank, S.K. 1985. Vein formation and distribution, Ohio and Mt. Baldy districts, Marysvale, Piute County, Utah, USA. *Mineralium Deposita*, **20**, 127-134.

Ohmoto, H. 1972. Systematics of sulfur and carbon isotopes in hydrothermal ore deposits. *Economic Geology*, **67**, 551-578.

Ohmoto, H. & Rye, R.O. 1979. Isotopes of sulfur and carbon. *In* Barnes, H.L. *ed. Geochemistry of hydrothermal ore deposits*. New York: Wiley Interscience, 509-567.

O'Neil, J.R., Clayton, R.N. & Mayeda, T.K. 1969. Oxygen isotope fractionation in divalent metal carbonates. *Journal of Chemical Physics*, **51**, 5547-5558.

Park, B.K. 1989. Potassium-argon radiometric ages of volcanic and plutonic rocks from the Barton Peninsula, King George Island, Antarctica. *Journal of Geological Society of Korea*, **25**, 495-497.

Park, M.E. 1991. Epithermal alteration and mineralization zoning within the stratovolcano, Barton Peninsula, King George Island. *Korean Journal of Polar Research*, **2**, 141-154.

Potter, R.W., III, Clynne, M.A. & Brown, D.L. 1978. Freezing point depression of aqueous sodium chloride solutions. *Economic Geology*, **73**, 284-285.

Robie, R.A., Hemingway, B.S. & Fisher, J.R. 1978. Thermodynamic properties of minerals and related substances at 298.15K and one bar (10^5 Pascals) pressure and at higher temperatures. *U.S. Geological Survey Bulletin*, No. 1452, 456pp.

Roedder, E. 1984. *Fluid inclusions*. (Reviews in Mineralogy, Volume 12). New York: Mineralogical Society of America, 644pp.

Rye, R.O. 1966. The carbon, hydrogen, and oxygen isotopic compositions of hydrothermal fluids responsible for the lead-zinc deposits at Providencia, Zacatecas, Mexico. *Economic Geology*, **61**, 1339-1427.

Rye, R.O., Bethke, P.M. & Wasserman, M.D. 1989. Diverse origins of alunite and acid-sulfate alteration: Stable isotope systematics. *U.S. Geological Survey Open-File Report*, **89-5**, 33pp.

Shikazono, N. 1972. Estimation of total sulfur in the ore-forming solutions. *Koshogakunote [Notes on ore geneisis, Tokyo]*, No. 12, 1-10. [in Japanese.]

Sillitoe, R.H. & Gappe, I.M. 1984. *Philippine porphyry copper deposits: geologic setting and characteristics*. Tech. Pub. 14. Bangkok: CCOP, 89pp.

Smellie, J.L., Pankhurst, R.J., Thomson, M.R.A. & Davies, R.E.S. 1984. The geology of the South Shetland Islands: VI. Stratigraphy, geochemistry and evolution. *British Antarctic Survey Scientific Reports*, No. 87, 85pp.

Stoffregen, R. 1985. *Genesis of acid-sulfate alteration and Au-Cu-Ag mineralization at Summitville, Colorado*. Ph.D. thesis, University of California (Berkeley), 204pp. [Unpublished.]

Taylor, H.P. Jr. 1974. The application of oxygen and hydrogen isotope studies to problems of hydrothermal alteration and ore deposition. *Economic Geology*, **69**, 843-883.

Taylor, H.P. Jr. 1973. O^{18}/O^{16} evidence for meteoric-hydrothermal alteration and ore deposition in the Tonopah, Comstock Lode, and Goldfield mining districts, Nevada. *Economic Geology*, **68**, 747-764.

Tokarski, A.K. 1987. Report on geological investigations of King George Island, South Shetlands (West Antarctica). *Studia Geologica Polonica*, **13**, 123-130.

Truesdell, A.H. & Hulston, J.R. 1980. Isotopic evidence on environments of geothermal systems. *In* Fritz, P. & Fontes, J.Ch. *eds. Handbook of environmental isotope geochemistry. The terrestrial environment*. Amsterdam: Elsevier, 179-226.

Truesdell, A.H., Nathenson, M. & Rye, R.O. 1977. The effects of subsurface boiling and dilution on the isotopic compositions of Yellowstone thermal waters. *Journal of Geophysical Research*, **82**, 3694-3704.

Watts, D.R. 1982. Potassium-argon ages and paleomagnetic results from King George Island, South Shetland Islands. *In* Craddock, C. *ed. Antarctic Geoscience*. Madison: University of Wisconsin Press, 255-261.